

Synergistic effect of polyethylene glycol 600 and polysorbate 20 on corrosion inhibition of zinc anode in alkaline batteries

Man Liang · Hebing Zhou · Qiming Huang ·
Shejun Hu · Weishan Li

Received: 8 December 2010 / Accepted: 29 May 2011 / Published online: 11 June 2011
© Springer Science+Business Media B.V. 2011

Abstract Polyethylene glycol 600 (PEG 600) and polysorbate 20 (Tween 20) were used as a composite corrosion inhibitor of zinc in alkaline solution for the first time. The effects of the composite and individual inhibitors on corrosion inhibition of zinc were evaluated by weight-loss analysis and electrochemical methods including potentiodynamic, potentiostatic, and electrochemical impedance spectroscopic measurements. It was found that there was a synergistic effect between PEG 600 and Tween 20 on corrosion inhibition of zinc. The corrosion inhibition efficiency of the composite inhibitor, 500 ppm PEG 600 + 500 ppm Tween 20, was 89%, much higher than that of the individual inhibitor, 1000 ppm Tween 20 (71%) or 1000 ppm PEG 600 (55%). The battery (Zn/MnO₂) discharge performance tests showed that the composite inhibitor reduced the self-discharge of zinc anode more effectively than the individual inhibitor. The synergistic

mechanism between PEG 600 and Tween 20 was discussed.

Keywords Zinc · Corrosion inhibition · Inhibitor · Synergistic effect · Alkaline battery

1 Introduction

Zinc has been used as anode materials for several alkaline batteries, such as zinc-manganese dioxide, zinc-nickel hydroxide, zinc-silver oxide, and zinc-air, because it has many advantages including high specific energy, low equilibrium potential, low cost, and non-toxicity [1–3]. Owing to its high activity, zinc tends to be corroded in alkaline solution, resulting in inevitable capacity loss of the batteries. The most effective way to solve this problem is to introduce corrosion inhibitors to the electrolyte solution [4–8]. In the past, mercury was used as a successful inhibitor because it can enhance the over-potential of hydrogen evolution and thus inhibit the corrosion of zinc. Since mercury is now forbidden to be used in batteries due to its toxicity, environment-friendly substitutes for mercury need to be developed [9, 10].

Surfactants have been regarded as the promising substitutes for mercury in alkaline zinc batteries. Structurally, surfactant consists of two parts: polar group and non-polar group [11]. The polar groups of surfactants are adsorbed on while the non-polar groups escape from the surface of zinc to form a protective layer that inhibits the corrosion of zinc [12, 13]. The adsorption of surfactants affects not only cathodic reaction (hydrogen evolution) but also anodic reaction (zinc dissolution) on zinc electrode in alkaline batteries. Therefore, the surfactants that can inhibit the cathodic reaction but have less influence on the anodic

M. Liang · Q. Huang · S. Hu · W. Li
School of Chemistry and Environment, South China Normal
University, Guangzhou 510006, China

H. Zhou · W. Li
School of Materials Science and Engineering, South China
University of Technology, Guangzhou 510641, China

M. Liang · H. Zhou · Q. Huang · S. Hu · W. Li
Key Laboratory of Electrochemical Technology on Energy
Storage and Power Generation of Guangdong Higher Education
Institutes, South China Normal University, Guangzhou 510006,
China

M. Liang · H. Zhou · Q. Huang · S. Hu · W. Li (✉)
Engineering Research Center of Materials and Technology
for Electrochemical Energy Storage (Ministry of Education),
South China Normal University, Guangzhou 510006, China
e-mail: liwsh@scnu.edu.cn

reaction are believed to be effective for the application in alkaline zinc batteries.

Several surfactants have been used as corrosion inhibitors of zinc in alkaline solution and the surfactants containing polyoxyethylene group are believed to be more effective than other surfactants [14–17]. However, the corrosion inhibition of zinc by individual surfactant is unsatisfactory. So far, few investigations have been reported on the effect of the composite surfactants on corrosion inhibition of zinc. In this study, two environment-friendly surfactants, polyethylene glycol 600 (PEG 600) and polysorbate 20 (Tween 20), were combined as a composite inhibitor and its inhibition efficiency for zinc corrosion was compared with that of individual PEG 600 or Tween 20. PEG 600 and Tween 20 are nontoxic and biodegradable. As shown in Fig. 1, PEG 600 is a symmetric and linear molecule, while Tween 20 is an asymmetric and highly branched molecule. The composite of these two surfactants can be expected to exhibit better effect than the individual on corrosion inhibition of zinc.

2 Experimental

2.1 Weight loss measurements

Zinc samples for weight loss measurements were prepared as reported in references [4, 18, 19]. Zinc sheets (99.9985%, $7 \times 7 \times 0.24 \text{ mm}^3$) were immersed in 3.6 wt% dilute hydrochloric acid under ultrasonication for 5 min to remove the surface oxide that was formed in air during transportation, rinsed with doubly distilled water and degreased with acetone. After dried in vacuum and then weighted, the zinc sheets were immersed in 3 M KOH solutions containing PEG 600 and/or Tween 20 with various concentrations from 200 to 1000 ppm at room temperature for 1 day. Then the zinc sheets were washed with doubly distilled water and acetone, dried in vacuum and weighted accurately. The weight loss was obtained.

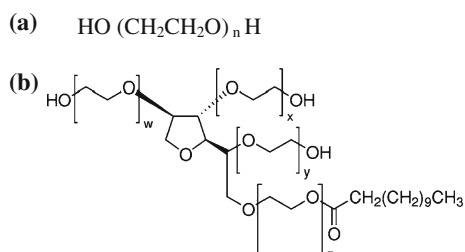


Fig. 1 Molecular structures of PEG 600 (a) and Tween 20 (b). $n = 13$, $x + y + z + w = 20$

Tween 20 and PEG 600 were purchased from Alfa Aesar and used without further treatment. Their polarity was indicated in terms of their dipole moments which were obtained by optimizing their molecular structures with HF/STO-3G method [20–22].

2.2 Electrochemical measurements

All electrochemical measurements were performed with PGSTAT-30 (Autolab, Eco Chemie, Netherlands) in a three-electrode cell at room temperature. The working electrode was a zinc (99.9985%) microdisk electrode embedded in an epoxy holder, having an exposed surface with a diameter of 1 mm. The counter electrode was a platinum sheet with a large surface area and the reference electrode was an Hg/3 M KOH/HgO electrode. All the potentials in this article were referred to this reference electrode. Prior to each experiment, the working electrode was polished with water proof silicon carbide paper (grits 400/p800–800/P2400), and then with aluminum oxide powder ($0.05 \mu\text{m}$) until a mirror-like surface was obtained. Finally, the electrode was cleaned in doubly distilled water and degreased in acetone under ultrasonication. To get rid of any oxide film on the surface, the working electrode was held at -1600 mV for 10 min before measurement. The electrolyte solution was 3 M KOH, which is more dilute than that (about 8 M) used in commercial zinc batteries. The dilute KOH solution was used in weight loss and electrochemical measurements in this study, because the electrochemical behavior of zinc in the KOH solution with different concentrations is similar and a dilute solution is less corrosive and easier to operate than a concentrated solution [23].

2.2.1 Potentiodynamic measurements

To obtain the corrosion current of zinc, Tafel plots were obtained in the potential range of -200 to $+200 \text{ mV}$ with respect to the open circuit potential (OCP) of zinc electrode at a scan rate of 1 mV s^{-1} .

To understand the polarization behavior of zinc electrode qualitatively, anodic and cathodic polarization curves were obtained individually at a scan rate of 20 mV s^{-1} . The potential was swept from the OCP to -2000 mV for cathodic polarization while from the OCP to -1000 mV for anodic polarization.

2.2.2 Potentiostatic measurements

Potentiostatic polarization measurements were carried out to understand the hydrogen evolution reaction on zinc. The potential was set at -1800 mV which only hydrogen evolution reaction took place.

2.2.3 Electrochemical impedance spectroscopy

The electrochemical impedance spectra were also obtained at -1800 mV for the understanding of hydrogen evolution reaction on zinc. In the electrochemical impedance spectroscopy measurements, the frequencies were 100 kHz to 0.01 Hz with the alternative current of ± 5 mV.

2.3 Battery performance determination

AG 13 Zn/MnO₂ button batteries were assembled by using electrolytic manganese dioxide, zinc powder, and separator (all these materials were provided by Zhaoqing Zhaohua Electronics Technology Co., Ltd.). The electrolyte was 8 M KOH solutions without and with 1000 ppm PEG 600, 1000 ppm Tween 20, and 500 ppm Tween 20 + 500 ppm PEG 600. The discharge performance of the batteries was measured on an instrument (Land CT2001A System, China) at 10 mA.

3 Results and discussion

3.1 Weight loss

3.1.1 Effect of inhibitors on inhibition efficiency

Table 1 presents the results obtained by weight loss measurements. The corrosion inhibition efficiency (η_w) was obtained based on [24]:

$$\eta_w = (\Delta W_1 - \Delta W_2) / \Delta W_1 \quad (1)$$

where ΔW_1 and ΔW_2 are the weight loss of zinc sheets after immersion in 3 M KOH solutions without and with inhibitors, respectively.

It can be seen from Table 1 that PEG 600 and/or Tween 20 can prevent zinc from corrosion to different extents. The inhibition efficiency of the inhibitors with the same concentration is always in the order of: Tween 20 + PEG 600 > Tween 20 > PEG 600, indicating that there is a synergistic effect between Tween 20 and PEG 600.

3.1.2 Adsorption isotherm

The degree of surface coverage (θ) of the inhibitors on zinc was obtained based on [18]:

$$\theta = \eta_w / 100$$

Figure 2 presents the adsorption isotherm curves of PEG 600 and/or Tween 20 on zinc. It can be found from Fig. 2 that there is a linear relationship between the concentration (c) of inhibitor and c/θ . The obtained slopes of the straight lines by fitting are about 1 (Table 2), indicating that the

Table 1 Weight loss of zinc in 3 M KOH solutions containing various inhibitors and the corresponding corrosion inhibition efficiencies and surface coverage rates

Inhibitor	ΔW (mg)	η_w (%)	θ
Free	1.91 ± 0.02	–	–
PEG 600 (ppm)			
200	1.11 ± 0.04	20.4	0.20
400	1.22 ± 0.03	35.7	0.36
600	1.01 ± 0.04	46.9	0.47
800	0.89 ± 0.02	53.0	0.53
1000	0.81 ± 0.02	57.2	0.57
Tween 20 (ppm)			
200	1.24 ± 0.02	34.8	0.35
400	0.81 ± 0.03	57.4	0.57
600	0.58 ± 0.03	69.7	0.70
800	0.55 ± 0.04	71.0	0.71
1000	0.52 ± 0.04	72.5	0.73
Tween 20 + PEG 600 (ppm)			
200	0.63 ± 0.02	66.7	0.67
400	0.53 ± 0.02	71.9	0.72
600	0.25 ± 0.02	87.0	0.87
800	0.23 ± 0.03	88.0	0.88
1000	0.22 ± 0.02	89.7	0.89

adsorption of the inhibitors obeys the Langmuir’s adsorption isotherm [19]:

$$\frac{c}{\theta} = \frac{1}{K} + c$$

where K is the adsorption equilibrium constant. It can be seen from Table 2 that the K value of Tween 20 is larger than that of PEG 600, suggesting that Tween 20 is adsorbed on zinc preferably. The K value of Tween 20 + PEG 600 is larger than that of individual Tween 20 or PEG 600, indicating that more species are adsorbed on zinc in the solution containing the composite inhibitor.

3.2 Electrochemical properties

Figure 3 presents the Tafel plots of zinc in 3 M KOH solutions containing various inhibitors. The corresponding electrochemical parameters derived from Fig. 3 are listed in Table 3. The corrosion current (I_{corr}) was determined by the extrapolation of the cathodic and anodic Tafel lines to the corrosion potential (E_{corr}). The corrosion inhibition efficiency (η_p) was obtained based on [25]:

$$\eta_p = (I_{\text{corr}} - I'_{\text{corr}}) / I_{\text{corr}} \quad (2)$$

where I_{corr} and I'_{corr} are the corrosion current of zinc in 3 M KOH solutions without and with inhibitors, respectively. It can be seen from Table 3 that the inhibition

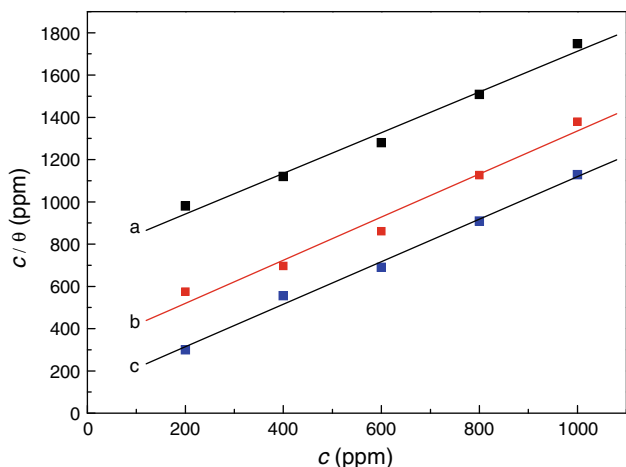


Fig. 2 Adsorption isotherms of (a) PEG 600, (b) Tween 20, and (c) Tween 20 + PEG 600 on zinc in 3 M KOH solutions. The surface coverage rates were obtained based on weight loss measurements

Table 2 Parameters of c/θ – c relationship for zinc in 3 M KOH solutions containing various inhibitors

Inhibitor	Linear correlation coefficient (r)	Slope	K (ppm ⁻¹)
PEG 600	0.986	0.96	0.0013
Tween 20	0.976	1.02	0.0031
Tween 20 + PEG 600	0.993	1.01	0.0088

efficiencies of the inhibitors are in agreement with those obtained from weight loss measurements (Table 1), confirming the synergistic effect between PEG 600 and Tween 20.

It can be seen from Fig. 3 that the inhibitors reduce both anodic and cathodic current. This indicates that the inhibitors can inhibit both the anodic and cathodic processes for

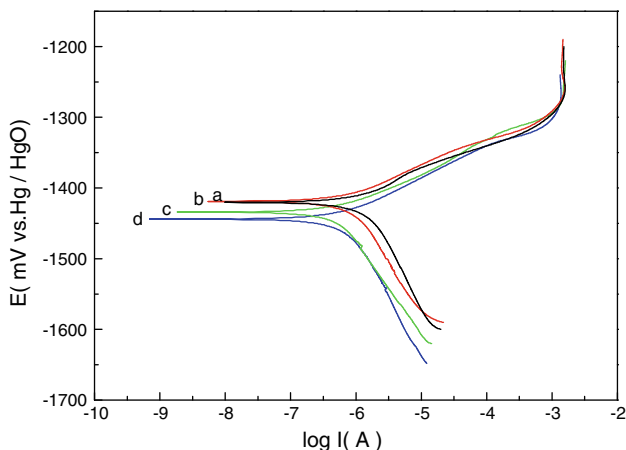


Fig. 3 Tafel plots of zinc in 3 M KOH solutions: (a) inhibitor free, (b) 1000 ppm PEG 600, (c) 1000 ppm Tween 20, (d) 500 ppm Tween 20 + 500 ppm PEG 600. Scan rate 1 mV s⁻¹

Table 3 Electrochemical parameters of zinc derived from the Tafel polarization curves of Fig. 3

Inhibitor	E_{corr} (mV)	I_{corr} (μA cm ⁻²)	η_p (%)
Free	-1420 ± 3	200 ± 3	–
1000 ppm PEG 600	-1422 ± 5	88 ± 2	55.3
1000 ppm Tween 20	-1434 ± 5	58 ± 1	70.9
500 ppm Tween 20 + 500 ppm PEG 600	-1443 ± 2	22 ± 1	89.2

zinc corrosion. It should be noted that the introduction of the inhibitors into the solution causes a negative shift of the corrosion potential. The change of the corrosion potential follows [26]:

$$\Delta\phi_{\text{corr}} = \frac{b_a b_c}{b_a + b_c} \lg\left(\frac{f_c}{f_a}\right) \quad (3)$$

where b_a and b_c are the anodic and cathodic Tafel slopes and f_a and f_c are the effect coefficients of inhibitors on anodic and cathodic processes of metal corrosion. The negative shift of corrosion potential suggests that the cathodic process is inhibited to a greater extent than the anodic process. It can be expected that the inhibitors, Tween 20 and/or PEG 600, can inhibit the zinc corrosion but affect hardly the discharge process of zinc as the anode of batteries.

Figure 4 presents the cathodic polarization curves of the zinc electrode in 3 M KOH solutions with various inhibitors. The hydrogen evolution reaction on zinc is polarized to different extents by three inhibitors. The polarization by Tween 20 is stronger than by PEG 600, while the polarization by PEG 600 + Tween 20 is stronger than by Tween 20, indicative of the synergistic effect between PEG 600 and Tween 20.

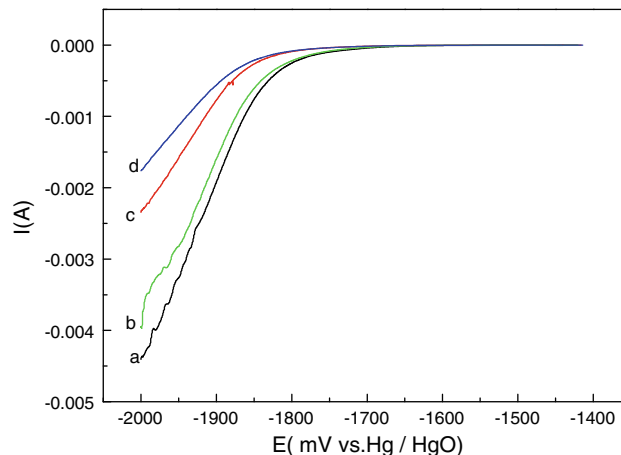


Fig. 4 Cathodic polarization curves of zinc in 3 M KOH solutions: (a) inhibitor free, (b) 1000 ppm PEG 600, (c) 1000 ppm Tween 20, (d) 500 ppm Tween 20 + 500 ppm PEG 600. Scan rate 20 mV s⁻¹

Figure 5 presents the anodic polarization curves of zinc electrode in 3 M KOH solutions with various inhibitors. The anodic dissolution reaction of zinc is also polarized by the inhibitors but the polarization of the anodic dissolution reaction is affected not so significantly as that of hydrogen evolution reaction. There is less difference in the polarization of the anodic dissolution reaction by three inhibitors. This suggests that the improvement of corrosion inhibition of zinc by the inhibitors is mainly ascribed to their effect on hydrogen evolution reaction. The inhibition of various inhibitors on hydrogen evolution reaction can be confirmed further by chronoamperometric and electrochemical impedance spectroscopic measurements.

Figure 6 presents the current–time curves of zinc in 3 M KOH solutions with various inhibitors at –1800 mV. The current for the hydrogen evolution reaction on zinc is in the order of: 500 ppm Tween 20 + 500 ppm PEG 600 < 1000 ppm Tween 20 < 1000 ppm PEG 600.

Figure 7 shows the Nyquist plots of zinc in 3 M KOH solutions with various inhibitors at –1800 mV. The Nyquist plots are capacitive arcs, indicating that the hydrogen evolution reaction on zinc is controlled by charge transfer step [27]. This reaction can be modeled by a Randles equivalent circuit, as shown by the inset of Fig. 7. In the equivalent circuit, R_s represents the solution resistance, R_{ct} represents the charge-transfer resistance and Q_{cdl} is a constant phase element (CPE) describing the interface double-layer. The solid lines in Fig. 7 are the fitting results by using the equivalent circuit and Table 4 presents element parameters obtained by fitting.

The corrosion inhibition efficiencies of various inhibitors can be obtained from the charge transfer resistance [28]:

$$\eta_R = (R_{ct} - R'_{ct})/R_{ct} \tag{4}$$

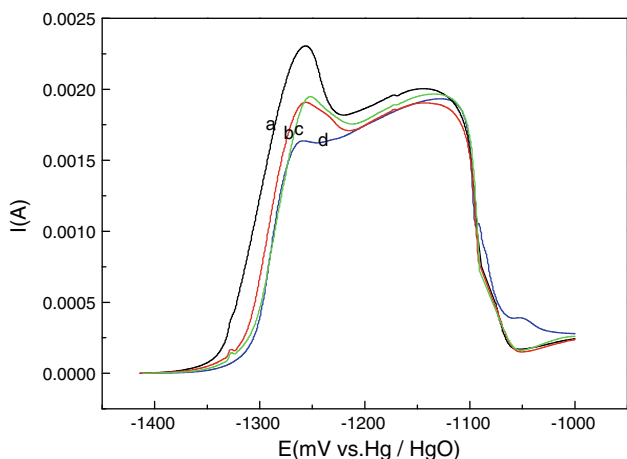


Fig. 5 Anodic polarization curves of zinc in 3 M KOH solutions: (a) inhibitor free, (b) 1000 ppm PEG 600, (c) 1000 ppm Tween 20, (d) 500 ppm Tween 20 + 500 ppm PEG 600. Sweep rate 20 mV s⁻¹

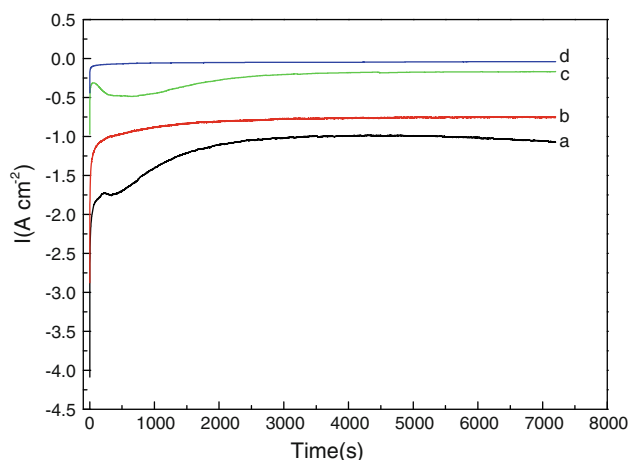


Fig. 6 Current–time curves of zinc in 3 M KOH solutions at –1800 mV: (a) inhibitor free, (b) 1000 ppm PEG 600, (c) 1000 ppm Tween 20, (d) 500 ppm Tween 20 + 500 ppm PEG 600

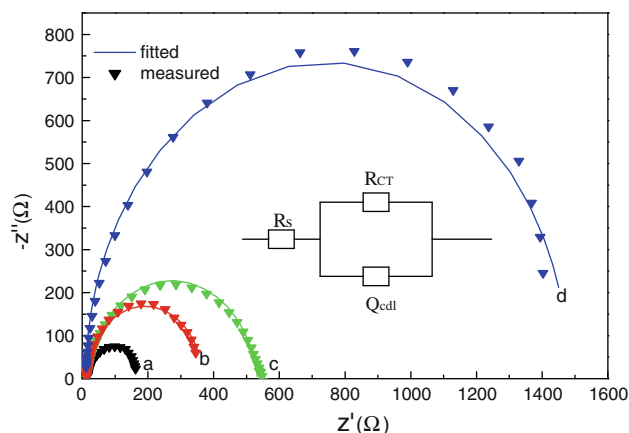


Fig. 7 Nyquist plots of zinc in 3 M KOH solutions at –1800 mV: (a) inhibitor free, (b) 1000 ppm PEG 600, (c) 1000 ppm Tween 20, (d) 500 ppm Tween 20 + 500 ppm PEG 600. The inset is the corresponding equivalent circuit

Table 4 Electrochemical impedance parameters for hydrogen evolution reaction on zinc at –1800 mV

Inhibitor	R_{ct} (Ω)	Q_{cdl}		η_R (%)
		Y_0 ($10^{-7} s^n \Omega^{-1}$)	n	
Free	156 ± 1	5.88 ± 0.23	0.96 ± 0.06	–
1000 ppm PEG 600	355 ± 3	5.04 ± 0.12	0.97 ± 0.03	55.9
1000 ppm Tween 20	521 ± 7	11.71 ± 0.71	0.92 ± 0.08	69.9
500 ppm Tween 20 + 500 ppm PEG 600	1471 ± 5	3.19 ± 0.05	0.88 ± 0.06	89.3

where R_{ct} and R'_{ct} are charge transfer resistance of zinc in 3 M KOH solutions with and without inhibitors, respectively. The obtained results are presented in Table 4. It can be seen that the η_R is in a good agreement with the η_p and the η_w . Since the charge transfer resistances are obtained at -1800 mV, which is very negative to the corrosion potential, only hydrogen evolution reaction takes place. The good agreement of the η_R with the η_p and the η_w confirms that the corrosion inhibition of zinc is accomplished mainly by the inhibition of hydrogen evolution reaction.

The synergistic effect can be ascribed to the different polarities of PEG 600 and Tween 20. The polarity of Tween 20 and PEG 600 can be indicated in terms of their dipole moments. Based on the theoretical calculation, the dipole moment is 4.40 D for Tween 20 (assuming $x = y = z = w = 5$. x , y , z , and w stand for the number of polyoxyethylene group in molecular structure as shown in Fig. 1b) and 1.85 D for PEG 600. The polarity of Tween 20 is stronger than that of PEG 600 and thus Tween 20 is adsorbed on zinc preferably. Zinc cannot be covered completely by Tween 20 due to the highly branched structure of Tween 20. The linear PEG 600 can be adsorbed on the remaining active sites, as shown in Fig. 8. Therefore, the composite is better than the individual.

3.3 Battery discharge performance

Figure 9 shows the constant current discharge curves of AG 13 button zinc-manganese dioxide batteries using various inhibitors after stored at 45 °C for 10 h. The stored discharge performance of the batteries is affected by the inhibitors. The inhibitors inhibit the self-discharge of anodic zinc, resulting in the improvement of the stored discharge capacity of the batteries. The battery using the

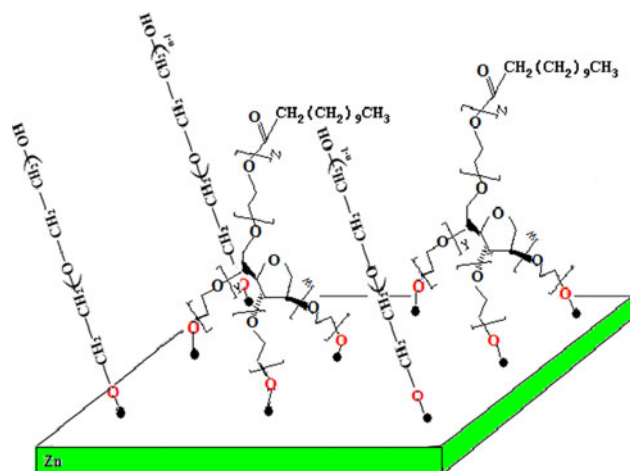


Fig. 8 Schematic adsorption of the composite inhibitor on zinc. Filled circle active sites

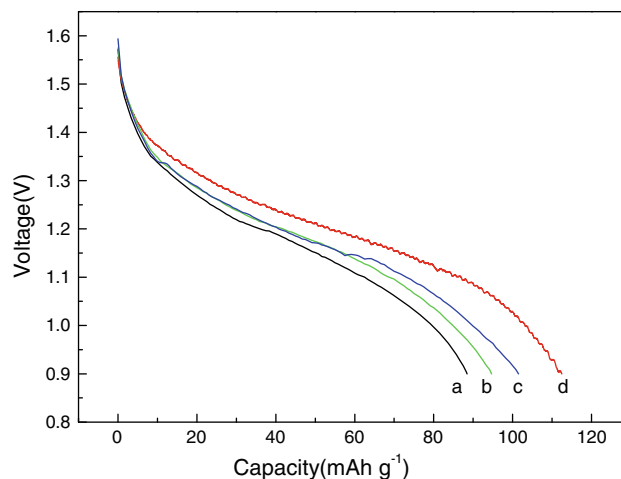


Fig. 9 Constant current (10 mA) discharge curves of AG 13 button zinc-manganese dioxide batteries using: (a) inhibitor free, (b) 1000 ppm PEG 600, (c) 1000 ppm Tween 20, (d) 500 ppm Tween 20 + 500 ppm PEG 600. The batteries were stored at 45 °C for 10 h before the discharge tests

composite inhibitor has the largest discharge capacity (120 mAh g^{-1}), confirming the synergistic effect between PEG 600 and Tween 20.

4 Conclusions

PEG 600 or Tween 20 can inhibit zinc corrosion to some extent mainly through inhibiting hydrogen evolution reaction. There is a synergistic effect between two inhibitors on zinc corrosion, because the corrosion inhibition efficiency of their composite is better than that of the individual inhibitor. The polarity of Tween 20 is stronger than that of PEG 600 and thus Tween 20 is adsorbed on zinc preferably. Zinc cannot be covered completely by Tween 20 due to the highly branched structure of Tween 20. The linear PEG can be adsorbed on the remaining active sites. The composite of PEG 600 and Tween 20 provides zinc battery with a promising substitute for mercury as inhibitor.

Acknowledgment This study is supported by Natural Science Foundation of Guangdong Province (Grant no. 10351063101000001).

References

- Huot JY, Malservisi M (2001) *J Power Sour* 96:133
- Wranglen G (1960) *Electrochim Acta* 2:130
- Skelton J, Serenyi R (1997) *J Power Sour* 65:39
- Shivkumar R, Kalaigan GP, Vasudevan T (1995) *J Power Sour* 55:53
- Wang JM, Qian YD, Zhang JQ et al (2000) *J Appl Electrochem* 30:113
- Sharma Y, Aziz M, Yusof J et al (2001) *J Power Sour* 94:129
- Cachet C, Stroeder U, Wiart R (1982) *Electrochim Acta* 27:903

8. Huot JY (1992) *J Appl Electrochem* 22:443
9. Zhou HB, Xu MQ, Huang QM et al (2009) *J Appl Electrochem* 39:1739
10. Zhou HB, Yang MZ, Li WS et al (2008) *Rare Metal Mat Eng* 37:404
11. Rosen MJ (1989) *Surfactant and interfacial phenomena*, 2nd edn. John Wiley, New York
12. Nmai CK (2004) *Cem Concr Compos* 26:199
13. Rusling JF (1997) *Coll Surf* 123:81
14. Ein-Eli Y, Auinat M, Starosvetsky D (2003) *J Power Sour* 114:330
15. Cohen-Hyams T, Ziengerman Y, Ein-Eli Y (2006) *J Power Sour* 157:584
16. Dobryszycski J, Bialozor S (2001) *Corros Sci* 43:1309
17. Zhu JL, Zhou YH, Gao CQ (1998) *J Power Sour* 72:266
18. Abiola OK, James AO (2010) *Corros Sci* 52:661
19. Deng SD, Li XH, Fu H (2011) *Corros Sci* 53:822
20. Petri A, Schwarz Th, Lentz A et al (1998) *J Mol Struc (Theochem)* 432:161
21. Dondela B, Peszke J, Slinwa W (2005) *J Mol Struc* 753:154
22. Li JC, Wang CL, Zhang WL et al (2002) *Acta Phys Sin* 51:776
23. Wang JM, Cao CN, Lin HC (1996) *J Chin Soc Corros Prot* 16:263
24. Singh AK, Quraishi MA (2010) Adsorption properties and inhibition of mild steel corrosion in hydrochloric acid solution by ceftobiprole. *J Appl Electrochem* 41(1):7
25. Deng SD, Li XH, Fu H (2011) *Corros Sci* 53:760
26. Cao CN, Zhang JQ (2002) *Introduction of electrochemical impedance spectroscopy*. Science Press, Beijing
27. Wilcox GD, Mitchell PJ (1989) *J Power Sour* 28:345
28. Cao CN (1996) *Corros Sci* 38:2073